CrossMark

ORIGINAL PAPER

Hydrogeochemical Characterization of Groundwater in and Around a Wastewater Irrigated Forest in the Southeastern Edge of the Tengger Desert, Northwest China

Peiyue Li[1,2] [ID] · **Jianhua Wu[1,2]** · **Hui Qian[1,2]** · **Yuting Zhang[1,2]** · **Nuan Yang[1,2]** · **Lijun Jing[1,2]** · **Peiyuan Yu[1,2]**

Abstract Groundwater is an essential part of water resources for human survival and economic development in arid regions over the world. Human activities and environmental change have imposed significant impacts on groundwater environment. To investigate the hydrogeochemical characteristics and evolution of groundwater in and around a desert region impacted by wastewater irrigation, 84 groundwater samples were collected and analyzed for 18 indices. Statistical and graphical approaches were applied to delineate the general hydrochemical characteristics of groundwater and the major factors influencing its evolution. Stable isotopes of ^{2}H and ^{18}O were applied to identify groundwater evaporation process. Hydrogeochemical modeling was also adopted to quantify the major reactions occurring in the groundwater system. The results reveal that the abundance of cations is $Na^+ > Ca^{2+} > Mg^{2+} > K^+$ for groundwater in the entire study area, while the abundance of anions for groundwater in the desert region is $HCO_3^- > Cl^- > SO_4^{2-}$, and that for groundwater in the alluvial plain is $HCO_3^- > SO_4^{2-} > Cl^-$. Groundwater chemistry in the study area is mainly of rock dominance, and dissolution/precipitation of minerals and cation exchange are major natural factors governing the formation of groundwater chemistry. However, stable isotopes and the occurrence of nitrate show that shallow groundwater evaporation and human activities also have some impacts on groundwater quality. Hydrochemical type transits from Ca–Cl to $HCO_3 \cdot SO_4$–Ca type, and then to $HCO_3 \cdot SO_4$–Ca·Mg type along the flow path. The transition is influenced by multiple factors with water–rock interactions the predominant one. The water–rock interactions for the upper and lower sections of the flow path, indicated by hydrogeochemical modeling, are different due to different geologic and hydrogeologic conditions.

Keywords Groundwater pollution · Water quality · Paper wastewater · Hydrogeochemical modeling · Tengger Desert

Introduction

Groundwater is indispensable for various uses such as supporting agriculture, enhancing economic expansion, and spurring urban growth (Schlager 2006). It is especially valuable in arid regions where there is only limited availability of precipitation and surface water resources (Li et al. 2015). Groundwater during the past several decades, however, is undergoing relative shortage in quantity because of increasing demand of water for human survival and economic development, and deterioration in quality due to human activities and natural environmental change (Vaux 2011; Li 2014). For instance, groundwater contamination and decline of water levels due to mismanagement and overexploitation have been reported in Jordan (El-Naqa and Al-Shayeb 2009), China (Han 1998; Wu and Sun 2015), USA (Ayotte et al. 2015; Rattray 2015), India (Ambast et al. 2006), Australia (McCallum et al. 2010), South Africa (Nel et al. 2009), and among many others.

Irrigated land has been raised in the arid zones around the world because of the increase in human population and

✉ Peiyue Li
  lipy2@163.com

[1] Key Laboratory of Subsurface Hydrology and Ecological Effects in Arid Region of the Ministry of Education, Chang'an University, No. 126 Yanta Road, Xi'an 710054, China

[2] School of Environmental Science and Engineering, Chang'an University, No. 126 Yanta Road, Xi'an 710054, China

🖄 Springer

associated agricultural production (Goyal and Tripathi 2016). The insufficiency of freshwater for uses and the incentive of environmental protection have driven users to adopt treated wastewater as an additional source of water supply for various purposes (Yang and Abbaspour 2007). Irrigation is the main consumer of the reclaimed wastewater, as it requires large volumes of water but has low requirement to the water quality. Irrigation with reclaimed wastewater has a long history in many countries such as in France (Tarchouna et al. 2010), Spain (Candela et al. 2007), South Korea (Jang et al. 2013), Cyprus (Christou et al. 2014), Egypt (Shurvilin et al. 2010), Israel (Kassa et al. 2005; Schacht and Marschner 2015), China (Li et al. 2014a; Wu et al. 2013), and India (Masto et al. 2009). Irrigation with reclaimed wastewater, however, has long been a controversial issue. On one hand, reclaimed wastewater, as an additional water resource, may help to save the valuable fresh water resources and the nutrients contained in the reclaimed wastewater such as nitrogen and phosphorus can improve soil fertility if used properly (Li et al. 2014a). Irrigation with reclaimed wastewater can also help to reduce investment in sewage treatment plants (Zhao 2010). Whereas, improper wastewater irrigation may have various potential adverse effects on the environment on the other hand. It may cause heavy metal contamination to soil and groundwater and alter soil physical properties and structures. For example, it may have hydrophobic effects on soil surfaces, reducing initial sorptivity and promoting the formation of preferential flow paths (Schacht et al. 2014). Therefore, great care should be taken when using reclaimed wastewater for irrigation, and scientific research must be conducted to guide the practice of wastewater irrigation.

Assessment and hydrogeochemical characterization of groundwater quality have been a hot topic for the past decades as the awareness of groundwater quality protection arise. A large number of literatures regarding groundwater quality assessment and hydrochemical characterization of groundwater have been published over the world (for example, Bouzourra et al. 2015; Brindha et al. 2014; Li et al. 2013a, 2014b; Qian et al. 2012a; Sajil Kumar et al. 2014; Vetrimurugan and Elango 2015; Wu et al. 2014, 2015). Recently, Li et al. (2012) developed an integrated groundwater quality assessment model based on rough set and Technique for Order Preference by Similarity to an Ideal Solution (TOPSIS). This integrated model reduced the number of parameters for assessment and enhanced the capability of grading of water quality. Rajesh et al. (2015) assessed the suitability of groundwater for domestic and irrigation purposes in a shallow weathered rock aquifer of Southern India. Sarikhani et al. (2015) assessed the hydrochemcial characteristics of groundwater on the basis of concentrations of major elements, and found that the dissolution of halite resulted in the linear increase in

sodium and chloride. The river recharge, dissolution of evaporated minerals intraformation, and agricultural returned water were responsible for groundwater salinity. There are also a limited number of literatures discussing the adverse impacts of wastewater irrigation on groundwater environment. For instance, Wang et al. (2008) and Li et al. (2007) reviewed the impacts of wastewater irrigation on groundwater, and proposed some measures to deal with the adverse effects. However, the mechanisms of contamination due to wastewater irrigation were not mentioned in their reviews. Kassa et al. (2005) investigated the differences in the impact of irrigation with freshwater and wastewater on groundwater quality in the Coastal Aquifer of Israel. Their research indicates that the composition of irrigation water, the lithology of unsaturated zone and land use are important factors determining the quality of the water that recharges groundwater (Kassa et al. 2005).

A forest covering over 100 km^2 has been built in the southeast edge of the Tengger Desert, China since 2005 for the purpose of treating wastewater from a paper making industry (MCC Meili Paper Industry Co., Ltd.) by irrigation and in turn producing raw materials for the paper production. This forest together with the sediments is considered as a constructed wetland for wastewater treatment and recycling (Wu et al. 2013). It is, however, a controversial issue and has attracted much attention from the public. Local residents living downstream of the forest are anxious, because the wastewater might flow toward the urban drinking water source zone, contaminating drinking water and risking human health. The impacts of wastewater irrigation on soil fertility and groundwater quality in this area have been reported (Li et al. 2014a; Wu et al. 2013). However, the hydrogeochemical characteristics of groundwater and its evolution under the effects of wastewater irrigation have never been reported till now. Therefore, the purposes of this study are (1) to investigate the hydrogeochemical characteristics of shallow groundwater in and around the wastewater irrigated region and (2) to determine the main factors governing groundwater chemistry by statistical techniques, stable isotopes, and geochemical modeling. This research will be helpful in supervising the practice of irrigation with reclaimed wastewater and in enhancing groundwater quality protection.
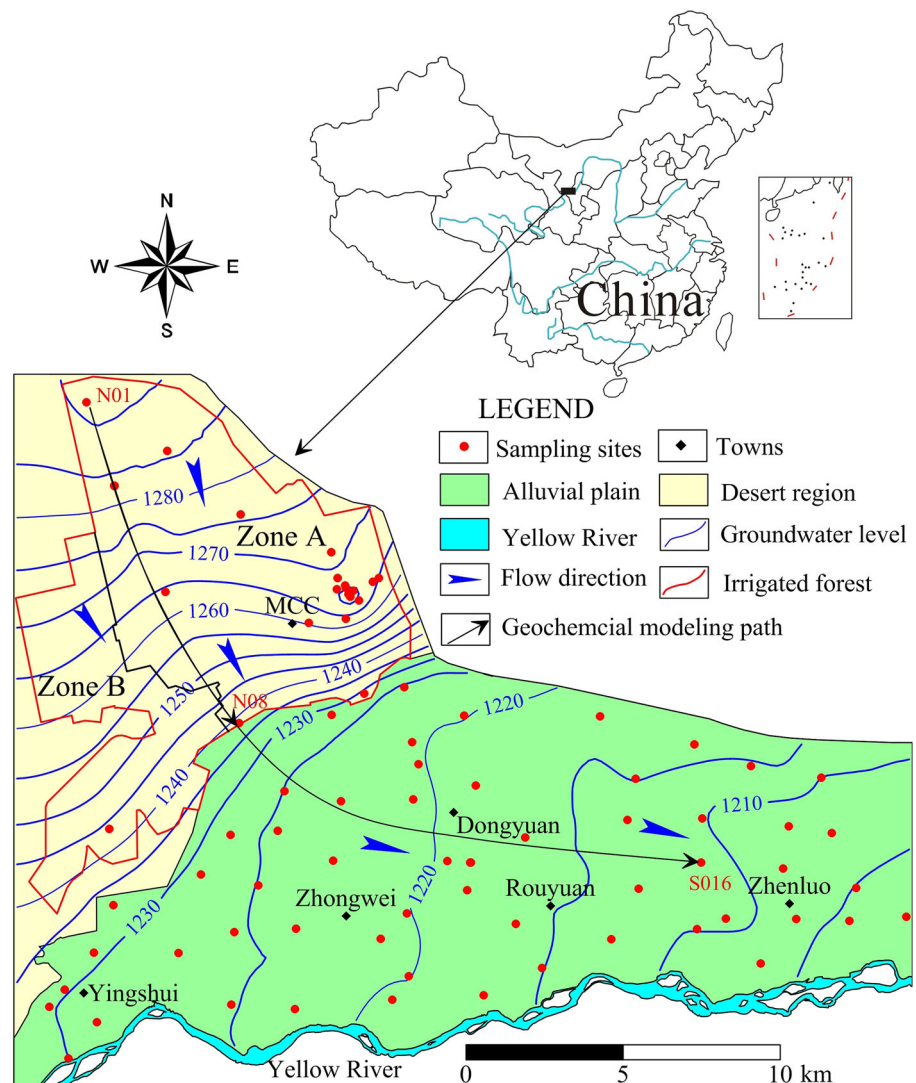
Study Area

Location and Climate

The study area is located in the western part of the Weining plain, the second largest alluvial plain in Ningxia Hui Autonomous Region. The study area, geographically

located between east longitude 105°04′–105°25′ and north latitude 37°27′–37°40′, covers about 400 km^2 in total and is divided into mainly two parts: the alluvial plain in the south and the desert region in the north (Fig. 1). The alluvial plain is formed by the Yellow River, the second largest river of China that runs through the study area from west to east along the southern boundary, while the desert region is part of the Tengger Desert that is formed mainly by wind. The forest established as part of the integrated forest-paper production system by the MCC Meili Paper Industry is located in the desert region. The integrated forest-paper production system uses paper wastewater to irrigate the forest after mixing with the Yellow River water in a ratio of 1:1, and the forest in turn provides raw materials for the paper production (Wu et al. 2013). The forest can be further divided into two subzones: the east zone irrigated with the mixed wastewater (Zone A in Fig. 1) and the west zone irrigated by pure Yellow River

water (Zone B in Fig. 1). The alluvial plain in the south of the study area is the main residential and agricultural region. The Zhongwei city and many towns are just situated in the plain and groundwater is the main source of water for domestic and industrial uses in the plain. A small portion of irrigation water also stems from groundwater. Therefore, groundwater is crucial for the survival of human beings and the development of economy in this study area.

As is located in the inland of China, the study area is far from the sea and is characterized by a continental arid monsoon climate with a dust-laden spring, a short and hot summer, a very short autumn, and a long and very cold winter (Qian et al. 2012a). Annual precipitation here is small and is only 179.4 mm. However, the annual evaporation rate in this area is 1828.6 mm, which is over ten times of the annual precipitation and makes this area quite deficit of local water resources. The rainfall mainly occurs in June to September, amounts to 73.6 % of the total

Fig. 1 Location of the study area and sampling sites

rainfall. Affected by global climate change, the study area is experiencing a rising temperature and a declining evaporation, but rainfall keeps relatively stable (Li 2014).

Hydrogeology

As silty clay is not present continuously over the study area, the entire study area is covered by single phreatic aquifer and there exist no confined aquifers here within the Quaternary layer (Li 2014; Zheng et al. 2014). According to borehole data, the Quaternary aquifer in the alluvial plain is usually less than 100 m in thickness. Gravels and sands are main media constituting the aquifer and loamy sands and silty clay form the aquitard. The permeability of the aquifer is relatively good with hydraulic conductivity ranging from 6 to 12 m/day. The aquifer located in the desert region is formed by fine sand, sand, and sandy clay, usually about 20 m in thickness. The permeability of the desert aquifer, with a hydraulic conductivity of 6 m/day, is smaller than that of the alluvial aquifer. Sand layer becomes thinner while gravel layer becomes thicker from northwest to southeast with the Yellow River approaches (Li 2014). According to our mineral analyses results, aquifer media in this area is rich in minerals such as dolomite, calcite, plagioclase (typically albite and anorthite), quartz, K-feldspar, gypsum, hornblende, illite, and chlorite. In addition, halite, montmorillonite, and kaolinite are also common in this area. With huge thickness and high permeability, aquifer in the alluvial plain can usually yield large volumes of groundwater for various uses (Zheng et al. 2014). It is estimated that the specific yield of wells ranges from 199.58 to 4845.31 m^3/day as per different locations of the wells (Li 2014, Zheng et al. 2014).

Controlled by hydrogeological conditions and macroscopic topographic features, groundwater flows from north to south in the desert region, and then changes its flow direction toward the east in the alluvial plain (Fig. 1). In addition to the natural factors such as geology, topography, geologic structures, meteorology, hydrology, and hydrogeology that primarily govern the patterns of groundwater recharge, runoff, and discharge, groundwater budget is also influenced by anthropogenic factors such as groundwater abstraction and irrigation (Zheng et al. 2014). Typically, groundwater in the study area gets recharge from precipitation, irrigation, canal leakage, and lateral inflow, while is discharged by evaporation, artificial extraction, drain discharge, and lateral outflow (Li et al. 2014b). Based on groundwater budget calculated for the period from August 2011 to July 2012 (Jin 2013), total groundwater recharge during this period amounts to 204 million m^3/a, while total groundwater discharge during the same period is 192 million m^3/a, indicating that groundwater level may be subject to slight rise in the near future under current

situations. Of the total groundwater recharge, canal leakage accounts for more than 66 %, irrigation infiltration amounts to 23 %, whereas lateral inflow and rainfall infiltration are of the order of 5 and 6 %, respectively (Jin 2013). With respect to the total groundwater discharge, evaporation, with 90 million m^3/a, accounts for the greatest proportion (46 %) followed by artificial abstraction which accounts for about 32 % of the total discharge. Discharges through drains and lateral outflow are relatively small, accounting for only 18 and 4 % of the total discharge, respectively (Jin 2013; Zheng et al. 2014).

Materials and Methods

Sample Collection and Analysis

For this study, 84 groundwater samples were collected from monitoring wells, hand-pumping wells, and boreholes in October, 2011 for physiochemical analysis. Sampling locations were recorded using a potable GPS device, and are shown in Fig. 1. Prior to sampling, all wells were pumped for several minutes to eliminate the influence from stagnant water. Samples were collected in 2.5 L plastic bottles which had been rinsed and washed 3–4 times using the water to be sampled. After sampling, samples were labeled, stored, and transported to the laboratory for physiochemical analysis. Analyzed indices include Na^+, K^+, Ca^{2+}, Mg^{2+}, Cl^-, HCO_3^-, SO_4^{2-}, NH_4-N, NO_3-N, NO_2-N, fluoride (F^-), total hardness (TH), total dissolved solids (TDS), pH, and chemical oxygen demand (COD_{Mn}). Among these indices, pH was measured in situ using a portable pH meter. Cl^-, SO_4^{2-}, HCO_3^-, and NH_4-N were determined by routine titrimetric methods. Na^+ and K^+ were determined by flame atomic absorption spectrometry, and Ca^{2+}, Mg^{2+}, and TH were measured by EDTA titrimetric method. TDS was determined by drying and weighing. Samples were dried at 105 °C and then weighed with an analytical balance capable of weighing to 0.1 mg. F^- was measured using the ion-selective electrode method. NO_3-N and NO_2-N were determined by Ion Chromatography. Standard procedures recommended by Rice et al. (2012) were followed to ensure the reliability of the analysis results. Duplicates were also performed during the analysis for quality assurance and quality control (QA/QC).

To quantify the impacts of evaporation on groundwater chemistry, 19 groundwater samples were collected for analysis of stable hydrogen and oxygen isotopes (^{2}H and ^{18}O). All of these isotopic samples were collected from shallow wells (typically less than 30 m in depth), and groundwater is considered to have probably undergone evaporation. Isotopic analyses of ^{18}O and ^{2}H were carried out at the State Key Laboratory of Environmental

Geochemistry, Institute of Geochemistry of Chinese Academy of Sciences. Duplicates were introduced in the analytical procedure for QA/QC. Isotopic ratios are expressed in per mil (δ).

Hydrogeochemical Modeling

Geochemical modeling is an important and useful tool for studying hydrochemical evolution mechanisms (Li et al. 2010). Inverse modeling is one of the most popular modeling approaches that have been adopted in various studies. In this paper, the PHREEQC (Parkhurst and Appelo 1999), a thermodynamic program, was applied to calculate saturation index (SI) and to perform the inverse geochemical modeling. To perform the modeling, the initial and final solutions (also known as end-member solutions) along a flow path must be first determined according to groundwater flow directions (Fig. 1). Inverse geochemical modeling is usually used to calculate the moles of minerals and gases that have dissolved in or precipitated/degassed from the solutions based on the rule of mass balance to explain the differences in compositions between the initial and final end-member solutions (Li et al. 2010; Parkhurst and Appelo 1999). The mass balance of the conceptual models can be expresses as follows (Li et al. 2010):

$$\sum_{j=1}^{n} a_{ij} x_j = b_i \tag{1}$$

where a_{ij} is the stoichiometric number of element i in mineral j, x_j is the molar number of minerals or gases that have dissolved or precipitated (degassed), and b_i represents the increment of element i in the final water solution compared with the initial water solution (Li et al. 2010). Positive values of mass transfer indicate dissolution of minerals or gas, whereas negative values indicate precipitation or outgassing.

Another important term that has been widely used in hydrogeochemical studies is the SI, which describes the trend of dissolution or precipitation for a given mineral. SI can be defined by the following formula (Li et al. 2010):

$$SI = \log \frac{IAP}{K} \tag{2}$$

where IAP represents the ion activity product of ions in a solution, and K is the equilibrium constant for a mineral at a certain temperature (Li et al. 2010). SI >0 indicates oversaturation and minerals may be subject to precipitation, SI <0 means under-saturation and minerals will dissolve, and SI = 0 suggests saturation and minerals are in equilibrium status with respect to the solution (Parkhurst and Appelo 1999). In the present study, the SI values for minerals concerned were calculated by PHREEQC.

Results and Discussion

General Groundwater Chemistry

Table 1 lists the statistical analysis results of the analyzed hydrochemical indices. Groundwater pH ranges from 7.00 to 8.86 in the desert region and is observed in the range of 7.14–8.18 in the alluvial plain, indicating neutral to slightly alkaline water over the study area. However, the mean groundwater pH in the desert region is higher than that in the alluvial plain, which may be explained by the percolation of paper wastewater whose pH typically ranges from 8.42 to 8.56. TDS and TH are important indicators of drinking water quality (WHO 2011). In this study, TDS and TH in the desert region are observed in the ranges of 298.45–4488.75 and 55.00–1780.14 mg/L, respectively, and those in the alluvial plain are, respectively, 604.00–3288.00 and 159.75–1979.17 mg/L (Table 1). The high salinity in the groundwater can be attributed to the dissolution of soluble salts and minerals, evaporation of groundwater as well as the infiltration of wastewater (Li 2014).

Cations and anions in groundwater show significant spatial variation in the study area. As shown in Table 1, the concentrations of Na^+, K^+, Ca^{2+}, and Mg^{2+} in the groundwater are observed in the ranges of 35.46–923.00, 1.00–91.70, 12.50–574.00, 8.34–216.20 mg/L, respectively. Na^+ has the highest abundance and followed by Ca^{2+} and Mg^{2+}, and K^+ has the lowest mean value. According to the mean values of cations, Na^+ concentration in the desert region (374.66 mg/L) is much higher than that in the alluvial plain (116.81 mg/L), because Na^+ concentration in the wastewater is very high and the infiltration of wastewater elevated the Na^+ concentration in groundwater in the desert region. The concentrations of HCO_3^-, SO_4^{2-}, and Cl^- in the study area range within 119.13–804.59, 3.39–2772.00, and 42.25–1131.14 mg/L with means of 446.55, 333.72, and 210.98 mg/L, respectively (Table 1). Because the Cl^- concentration in wastewater is high, its use as irrigation water results in the elevation of Cl^- in groundwater in the desert region. The concentration of SO_4^{2-} in the groundwater of the alluvial plain exceeds that in the desert region due to the intense evaporation of shallow groundwater in the alluvial plain. According to the means, the abundance of anions for groundwater in the desert region is $HCO_3^- > Cl^- > SO_4^{2-}$, and that for groundwater in the alluvial plain is $HCO_3^- > SO_4^{2-} > Cl^-$.

Fluoride (F^-) is an essential element for human health (Currell et al. 2011; Li et al. 2014c; Wu et al. 2015). According to the World Health Organization (WHO), water with F^- higher than 1.5 mg/L is unsuitable for

Table 1 Statistical analysis of groundwater samples

Region	Index	Unit	Sample no.	Min	Max	Mean	SD
Desert region	NH_4-N	mg/L	26	0.01	2.52	0.50	0.67
	NO_2-N	mg/L	26	0.00	0.44	0.07	0.11
	NO_3-N	mg/L	26	0.35	50.00	12.00	12.03
	Ca^{2+}	mg/L	26	12.50	356.40	72.12	75.81
	Mg^{2+}	mg/L	26	9.27	216.20	42.80	38.37
	Na^+	mg/L	26	35.46	923.00	374.66	246.79
	K^+	mg/L	26	4.91	91.70	19.13	23.92
	HCO_3^-	mg/L	26	119.13	804.59	427.42	203.66
	SO_4^{2-}	mg/L	26	3.39	1669.00	206.55	322.90
	Cl^-	mg/L	26	42.25	1131.14	346.02	216.76
	TDS	mg/L	26	298.45	4488.75	1358.17	897.10
	pH	mg/L	26	7.00	8.86	8.16	0.42
	COD_{Mn}	mg/L	26	0.44	36.50	7.79	9.53
	TH	mg/L	26	55.00	1780.14	329.39	317.34
	F^-	mg/L	26	0.38	21.10	4.31	5.11
Alluvial plain	NH_4-N	mg/L	58	0.02	3.72	0.13	0.52
	NO_2-N	mg/L	58	0.00	0.29	0.05	0.08
	NO_3-N	mg/L	58	0.08	137.00	14.83	25.98
	Ca^{2+}	mg/L	58	39.70	574.00	133.66	87.55
	Mg^{2+}	mg/L	58	8.34	148.00	74.94	29.39
	Na^+	mg/L	58	39.10	480.00	116.81	77.79
	K^+	mg/L	58	1.00	52.70	16.46	11.15
	HCO_3^-	mg/L	58	195.20	789.34	455.13	113.77
	SO_4^{2-}	mg/L	58	108.00	2772.00	390.73	476.55
	Cl^-	mg/L	58	57.40	678.00	150.44	118.17
	TDS	mg/L	58	604.00	3288.00	1153.53	580.22
	pH	mg/L	58	7.14	8.18	7.55	0.23
	COD_{Mn}	mg/L	58	0.60	4.40	1.37	0.66
	TH	mg/L	58	159.75	1979.17	646.03	288.13
	F^-	mg/L	58	0.19	4.90	1.13	1.11
Total	NH_4-N	mg/L	84	0.00	3.72	0.25	0.60
	NO_2-N	mg/L	84	0.00	0.44	0.06	0.09
	NO_3-N	mg/L	84	0.08	137.00	13.96	22.56
	Ca^{2+}	mg/L	84	12.50	574.00	114.61	88.40
	Mg^{2+}	mg/L	84	8.34	216.20	64.99	35.50
	Na^+	mg/L	84	35.46	923.00	196.62	192.04
	K^+	mg/L	84	1.00	91.70	17.29	16.10
	HCO_3^-	mg/L	84	119.13	804.59	446.55	146.79
	SO_4^{2-}	mg/L	84	3.39	2772.00	333.72	441.25
	Cl^-	mg/L	84	42.25	1131.14	210.98	178.93
	TDS	mg/L	84	298.45	4488.75	1216.87	694.74
	pH	mg/L	84	7.00	8.86	7.74	0.41
	COD_{Mn}	mg/L	84	0.44	36.50	3.35	6.04
	TH	mg/L	84	55.00	1979.17	548.03	330.20
	F^-	mg/L	84	0.19	21.10	2.12	3.30

human consumption due to health concern (WHO 2011). In the present study, the concentration of F^- in groundwater over the study area is in the range of 0.19–21.10 mg/L with a mean of 2.12 mg/L (Table 1), suggesting a noticeable health risk. Especially, the mean concentration of F^- is much higher in the desert region than that in the alluvial
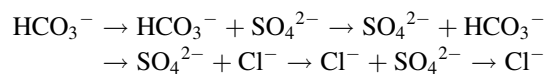
plain. The occurrence of F⁻ is regulated by hydrogeological conditions and geochemical environment, and its enrichment is usually favored in alkaline environment (Currell et al. 2011; Li et al. 2014c). COD indicates the amount of organic matter, and higher values mean organic pollution of groundwater. In this study, the concentration of COD in groundwater is much higher in the desert region than that in the alluvial plain, which shows the negative impacts of wastewater irrigation on groundwater quality.

Groundwater nitrate contamination is now very common and has become a globally growing problem in many regions of the world because of point and non-point sources (Esmaeili et al. 2014). Many researchers have reported serious groundwater nitrate pollution in China (Chen et al. 2007; Fang et al. 2015; Qian et al. 2015; Zhang et al. 2013). In this study, the concentration of NO_3-N in groundwater ranges within 0.08–137.00 mg/L with an average of 13.96 mg/L. Any value above 10 mg/L for nitrate is geochemically considered as pollution due to external factors (Karagüzel and Irlayici 1998). Therefore, groundwater is considered as seriously polluted by nitrate in the study area. NO_2-N and NH_4-N are also indicators of groundwater pollution. The ranges of their analyses vary within 0–0.44 and 0–3.72 mg/L, respectively (Table 1). It should also be noted that the concentrations of NH_4-N and NO_2-N in the desert region are greater than that in the alluvial plain as per their mean concentrations. However, because of different geological environments and a much longer history of fertilizer application in agriculture in the alluvial plain, groundwater nitrate pollution seems more severe in the alluvial plain than that in the desert region.

Durov diagram (Durov 1948) was generated to delineate the hydrochemical characteristics of groundwater (Fig. 2). Figure 2 reveals that about half of the water samples have TDS less than 1000 mg/L with HCO_3⁻ as the main anion. More than 35 % of the water samples are brackish water with TDS ranging from 1000 to 2000 mg/L. The concentrations of anions are close with each other for the brackish water, indicating mixed type of groundwater. A small portion of the water samples (ten samples) have TDS content greater than 2000 mg/L with high concentrations of SO_4^{2-} and Na^+. The TDS content in phreatic water varies spatially, and is closely related with the strong evaporation conditions and the quality of recharge water in the study area. Brackish water is usually found in the northeast regions of the study area where groundwater receives recharge from boundary inflow with high salinity. According to the Durov diagram (Durov 1948), groundwater in the study area is mainly of HCO_3–Ca·Mg, SO_4–Na, HCO_3·Cl–Na·Ca, and HCO_3·SO_4·Cl–Na·Mg types.

Hydrogeochemical Transition Along Flow Direction

With groundwater flowing from upstream to downstream, a series of water–rock interactions will occur in the aquifers, thereby increasing the ion contents in groundwater (Li 2014). In addition, ions in groundwater may also undergo slight increase due to the influences from human activity and groundwater evaporation. Therefore, it is crucial to investigate the hydrogeochemical transition of groundwater along the flow direction for gaining a better understanding of the role of water–rock interactions and other factors in regulating groundwater chemistry. Chebotarev (1955) have found, by a large number of studies, that the major anions in a regional groundwater system follow the below sequence along the groundwater flow (Qian and Li 2011):

$$HCO_3^- \rightarrow HCO_3^- + SO_4^{2-} \rightarrow SO_4^{2-} + HCO_3^- \\ \rightarrow SO_4^{2-} + Cl^- \rightarrow Cl^- + SO_4^{2-} \rightarrow Cl^-$$

In the present study, a flow path is determined according to the hydrogeological settings and groundwater flow direction (Fig. 1). This flow path reflects the changes of hydrochemistry in accordance with the geomorphology. Three representative sampling sites are selected in this path: N01, N08, and S016. N01 is the groundwater monitoring well located in the uppermost north of the forest irrigated by wastewater. S016 is a hand-pumping well located in the center of the alluvial plain, while N08 is a monitoring well located in the transition belt of the two landforms. Hydrochemical types and the variation of major ions along the flow direction are delineated in Fig. 3 by Piper and Stiff diagrams (Piper 1944; Stiff 1951).

As shown in Fig. 3, along the flow path, higher Cl⁻ concentration is observed than other anions and Ca^{2+} is the dominant cation in the upstream groundwater (Stiff diagram in Fig. 3), making it a Ca–Cl type for the upstream groundwater (Piper diagram in Fig. 3). With groundwater flowing downstream, the concentration of Cl⁻ decreases significantly and HCO_3⁻ increases sharply, while cations show only minor variation, resulting in a transition of water type to HCO_3·SO_4–Ca type in the transition belt of the landforms. With groundwater flowing further downstream to the alluvial plain, almost all ions show great increase in their absolute contents. A noticeable increase of Na^+, Mg^{2+}, and Ca^{2+} has been observed in the downstream, and SO_4^{2-} and HCO_3⁻ also increase a lot. The hydrochemical type of groundwater in the downstream of the flow path becomes HCO_3·SO_4–Ca·Mg type (Fig. 3).

Compared with the research results by Chebotarev (1955), it is found that the hydrogeochemical transition of groundwater in the study area does not follow the pattern revealed by Chebotarev (1955), because groundwater in the study area is influenced by local factors such as wastewater
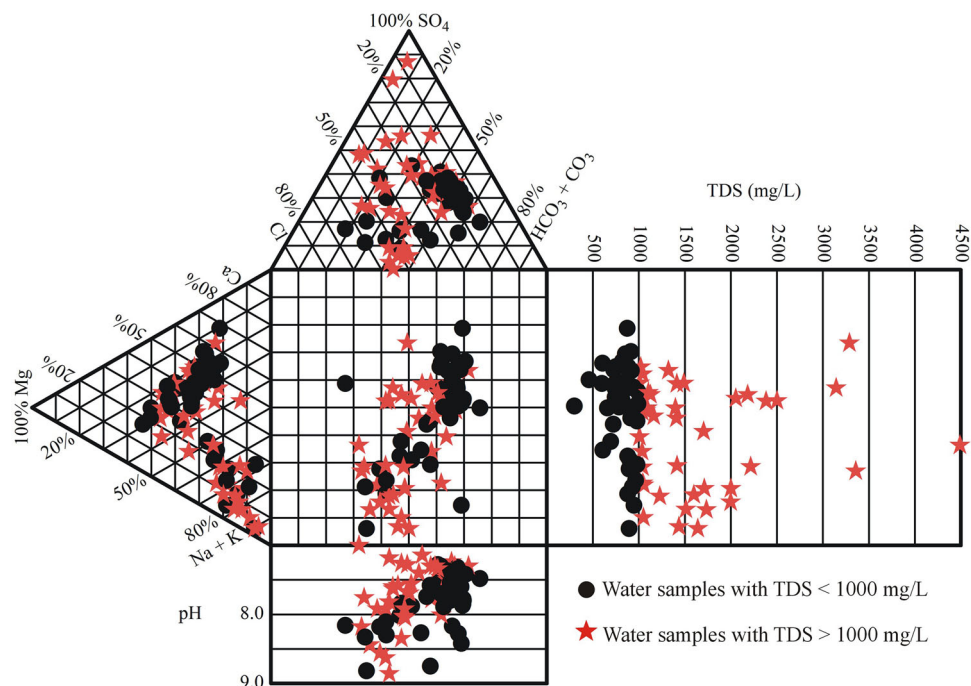
irrigation. There are generally three reasons that can
explain the sharp increase of HCO_3^- and the dramatic
decrease of Cl^- from N01 to N08. First, the irrigation of
the forest increases the groundwater flow rate, taking away
soluble salts (mainly Cl^-). Second, irrigation water for the
forest contains relatively high HCO_3^-, and third, ground-
water level depth is great in the forest region, making
groundwater evaporation minimal. From N08 to S016,
almost all ions show significant increase in their absolute
contents, which may be due to the shallow water depth in
the alluvial plain and strong groundwater evaporation. It is
also interesting to note that the hydrogeochemical transi-
tion of groundwater in the study area also differs from that
reported by Qian and Li (2011) in an adjacent plain with
similar climate, hydrogeology, and hydrology. Types and
extent of human interference to groundwater may be the
main responsible reason for the differences.

The above discussion indicates that tremendous chan-
ges in groundwater chemistry have occurred because of
long irrigation history and growing human activities in the
study area, in addition to water–rock interactions. The
spatial distribution of groundwater chemical compositions
has also been altered. This further demonstrates that for
the shallow groundwater environment in the study area,
its natural property of formation and evolution has already
been gradually weakened and human interference begins
to act as a significant role in influencing groundwater
quality.

Factors Governing Groundwater Chemistry

There are several factors that may be responsible for the
hydrogeochemical transition of groundwater chemistry.
Gaining a clear understanding of the main factors gov-
erning groundwater chemistry is important for various
purposes such as groundwater quality protection and
groundwater resources development. For studying the for-
mation mechanisms of water, Gibbs (1970) proposed the
well-known Gibbs diagrams (Fig. 4). The Gibbs diagrams
include two sub-diagrams. One represents the relationship
between TDS and the weight ratio of Na^+ versus
$(Na^+ + Ca^{2+})$, and the other one denotes the relationship
between TDS and the weight ratio of Cl^- versus
$(Cl^- + HCO_3^-)$. According to these diagrams, ground-
water formation mechanisms include three types: rock
dominance, evaporation dominance, and precipitation
dominance (Gibbs 1970; Li et al. 2013a).

As shown in Fig. 4, most of the samples are plotted in
the middle part of the diagrams, indicating that rock
weathering is the most important natural factor governing
groundwater evolution. This is evidenced by the study
results of Wu et al. (2008). A large amount of dissolvable
minerals and salts occurs in the sediments and these sedi-
ments are the results of parent rock weathering. The sol-
uble salts will enter groundwater along with the percolation
of irrigation water and precipitation. Furthermore, their
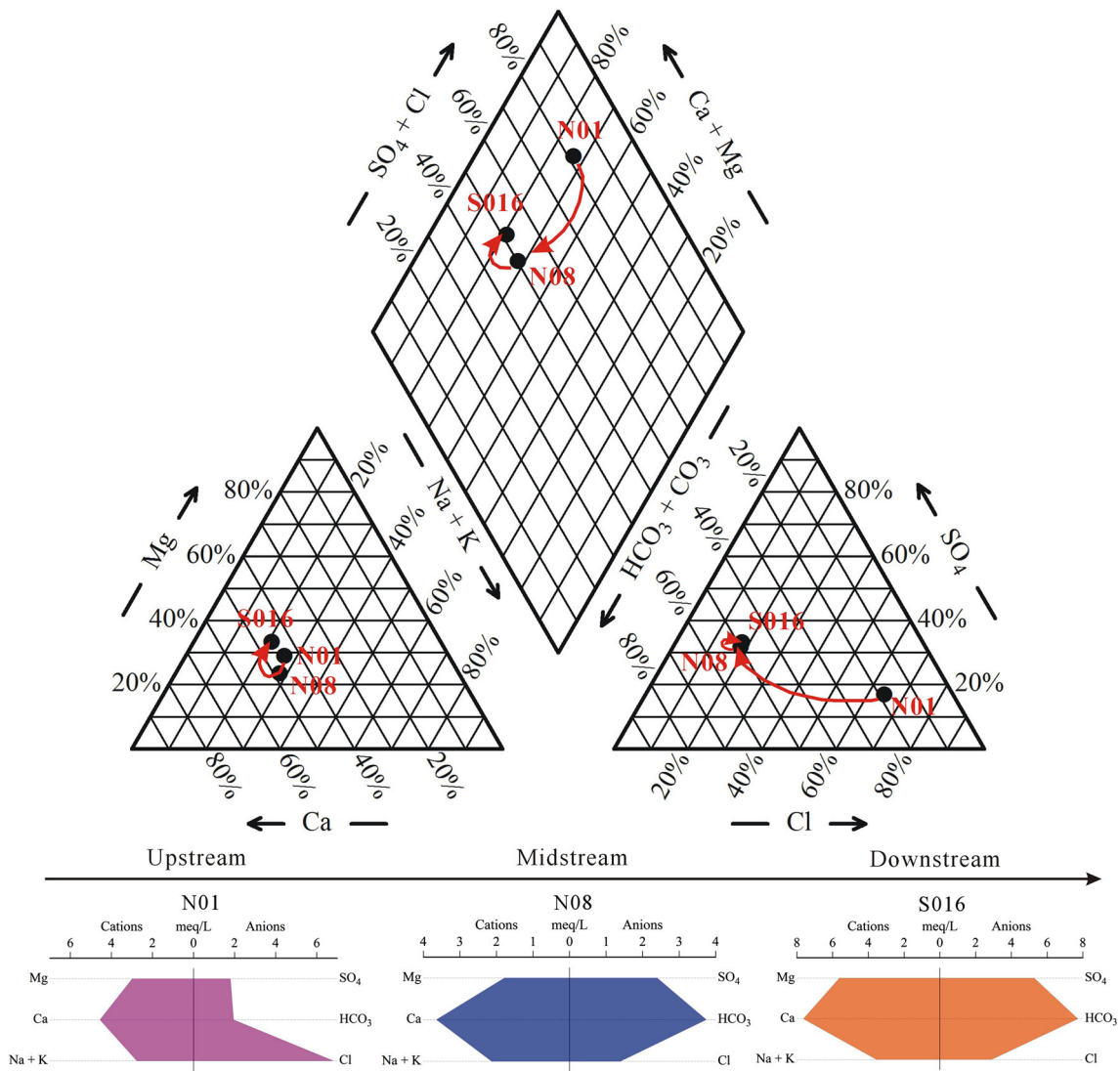isotopic investigation indicates that the regional ground-

Fig. 3 Piper and Stiff diagrams showing the transition of groundwater chemistry along the flow path

water in the alluvial plain was formed over 5000 years ago (Wu et al. 2008). The residence time is long enough to incur a variety of water–rock interactions including mineral dissolution. Figure 4 also shows that some samples are influenced, to some degree, by evaporation. This is happening where there is shallow groundwater level depth, especially in the alluvial plain. According to field investigation, groundwater level depth in many parts of the alluvial plain is small (typically less than 3 m). High evaporation rate and shallow groundwater level depth have resulted in intense groundwater evaporation over the alluvial plain, and groundwater chemistry is therefore influenced also by evaporation.

Gibbs diagrams are useful to analyze major natural factors governing groundwater formation mechanisms (Marghade et al. 2012; Naseem et al. 2010). However, they are unable to analyze the impacts of human activities on

groundwater chemistry, as the extent and degree of human activities are difficult to be quantified. Figure 4 suggests the major role of natural factors such as rock weathering and evaporation in the evolution of groundwater chemistry, but it does not necessarily mean that groundwater formation mechanisms are completely free from human interference. According to Li (2014), the impacts of human activities on the chemical compositions of groundwater can be divided into two categories: direct impacts and indirect impacts. Direct impacts of human activities are those that directly alter the contents of groundwater chemical compositions. On the contrary, indirect impacts do not alter the contents of groundwater chemical compositions directly, but they can indirectly influence the contents of groundwater chemical compositions by altering hydrodynamic conditions that may accelerate water–rock interaction processes and change groundwater evaporation intensity
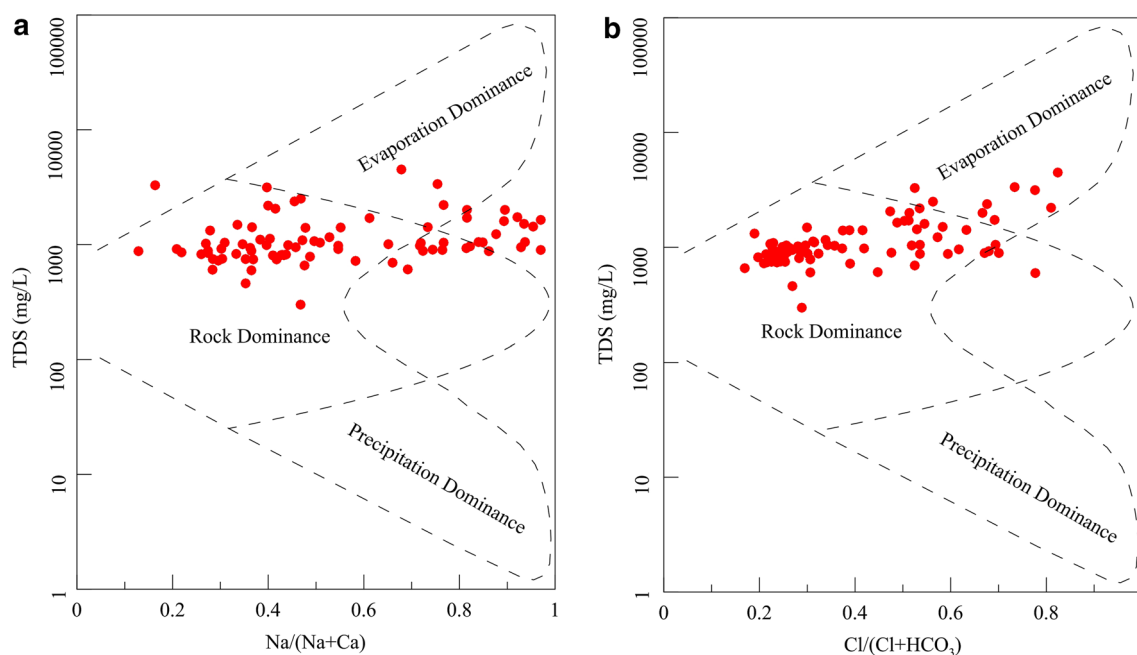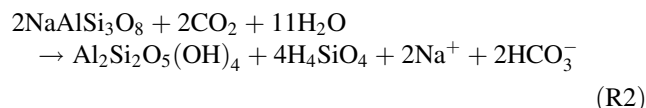
Fig. 4 Gibbs diagrams indicating general mechanisms of groundwater evolution

(Li 2014). For example, sewage infiltration can directly result in the increase of Cl^- and SO_4^{2-} in groundwater, thus sewage infiltration is considered as a direct impact. Groundwater abstraction will lower groundwater level, which may alter the hydraulic relationships of adjacent aquifers and/or enhance the water–rock interactions within the aquifers, forcing the variation in the contents of groundwater chemical compositions. There are many factors that can have indirect impacts on groundwater. Particularly, policies about the establishment of groundwater governance regulations and groundwater management framework can have indirect impacts on groundwater quality. The policies on economic development and population growth can also impact the groundwater quality indirectly. For instance, the revival of the Silk Road economic belt which is quite a hot topic in China and middle Asian countries can indirectly influence groundwater development and groundwater quality in these countries (Li et al. 2015). In the present study, chemical compositions of groundwater are influenced by rock weathering and groundwater evaporation, as indicated by the Gibbs diagrams. However, with the increase of impacts from human activities, traditional Gibbs diagrams show some limitations as they are unable to identify the anthropogenic impacts on groundwater formation.

Rock Weathering

To further refine the geochemical interpretation of rock weathering, some composition diagrams and correlation analysis were performed (Fig. 5; Table 2). This allows a

better understanding of the dominant water–rock interactions or source of the ions over the study area (Li et al. 2013b). Figure 5a shows that most samples are plotted along the 1:1 line, indicating that the dissolution of halite expressed as R1 is an important source of Na^+ and Cl^-. This is also evidenced by the SI of halite (Fig. 6) and the significant correlation between Na^+ and Cl^- (Table 2). Previous studies have shown that evaporite (such as halite) dissolution can contribute a large proportion of Na^+ and Cl^- to the water in the Yellow River drainage (Zhang et al. 2015). However, cation exchange between Na^+ and Ca^{2+} may be responsible for the deviation of plots from the 1:1. This will be discussed later. In addition, silicate hydrolysis may also add more Na^+, but not Cl^-, in groundwater, making Na/Cl ratio greater than unity (Li et al. 2014b). For example, the dissolution of albite can increase the concentration of Na^+ in groundwater, as expressed by R2.

$$NaCl \rightarrow Na^+ + Cl^- \qquad (R1)$$

$$2NaAlSi_3O_8 + 2CO_2 + 11H_2O$$
$$\rightarrow Al_2Si_2O_5(OH)_4 + 4H_4SiO_4 + 2Na^+ + 2HCO_3^- \qquad (R2)$$

Most of the samples are plotted along the 1:1 line of Ca^{2+} versus SO_4^{2-} graph (Fig. 5b), demonstrating that gypsum dissolution may be a contributing factor to these two ions in groundwater as expressed by R3 (Salem et al. 2015). Groundwater is under-saturated with respect to gypsum (Fig. 6) and thus gypsum can continue to dissolve in groundwater. However, some plots fall below the 1:1 line in Fig. 5b, which signifies that SO_4^{2-} may also result
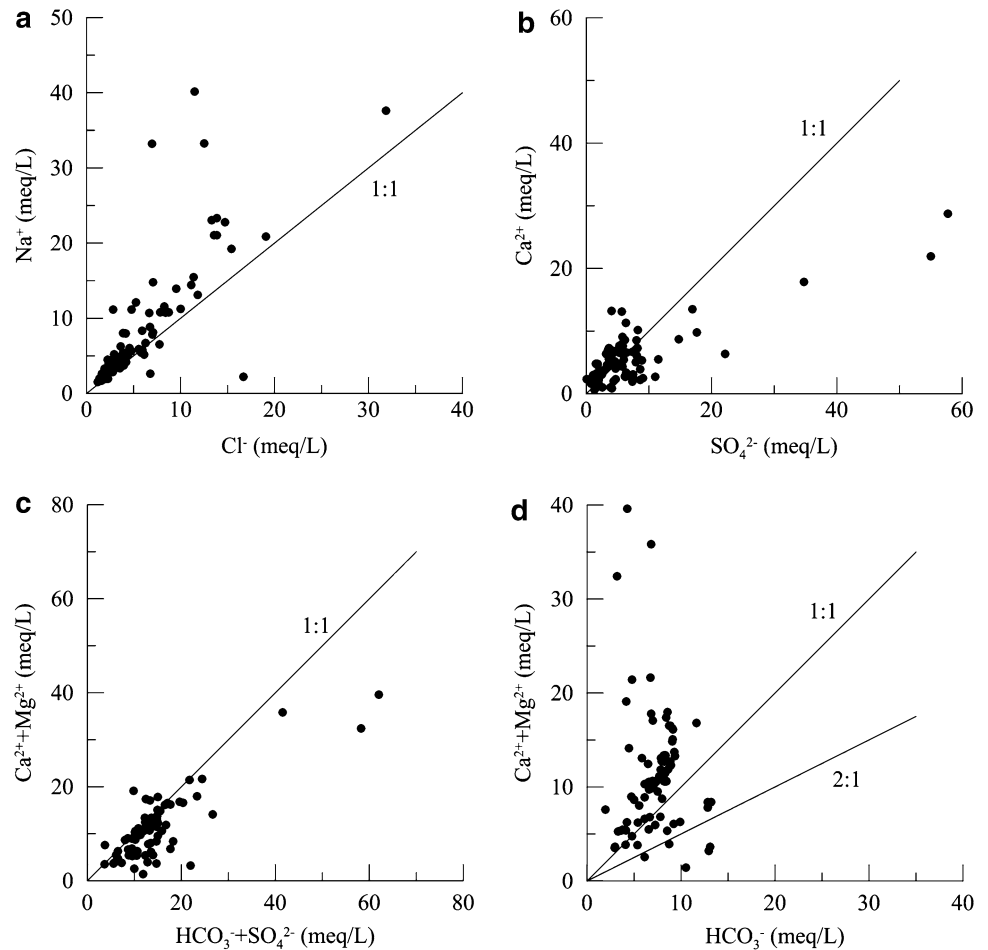
Fig. 5 Relationships between ions

Table 2 Pearson correlation for indices of collected groundwater samples

	NH$_4$-N	NO$_2$-N	NO$_3$-N	Ca^{2+}	Mg^{2+}	Na$^+$	K$^+$	HCO$_3^-$	SO$_4^{2-}$	Cl$^-$	TDS	pH	COD	TH	F$^-$
NH$_4$-N	1.00														
NO$_2$-N	**0.46**	1.00													
NO$_3$-N	−0.10	−0.03	1.00												
Ca^{2+}	−0.11	0.04	0.17	1.00											
Mg^{2+}	−0.10	−0.03	<u>0.27</u>	**0.58**	1.00										
Na$^+$	<u>0.22</u>	0.00	−0.02	0.00	0.04	1.00									
K$^+$	<u>0.24</u>	0.03	0.01	0.12	<u>0.24</u>	**0.31**	1.00								
HCO$_3^-$	<u>0.27</u>	−0.07	<u>−0.22</u>	−0.16	0.11	0.04	**0.34**	1.00							
SO$_4^{2-}$	−0.10	0.01	0.16	**0.81**	**0.60**	0.17	<u>0.24</u>	**−0.23**	1.00						
Cl$^-$	<u>0.24</u>	−0.02	0.06	0.09	0.18	**0.79**	0.21	0.14	**0.33**	1.00					
TDS	0.05	−0.07	<u>0.24</u>	**0.61**	**0.52**	**0.62**	**0.30**	0.06	**0.72**	**0.75**	1.00				
pH	<u>0.28</u>	<u>0.22</u>	0.04	**−0.45**	**−0.50**	**0.43**	0.06	**−0.32**	<u>−0.26</u>	0.18	−0.13	1.00			
COD	**0.61**	0.08	−0.06	−0.22	<u>−0.22</u>	**0.38**	**0.29**	**0.38**	−0.18	**0.39**	0.10	<u>0.22</u>	1.00		
TH	−0.10	−0.02	<u>0.23</u>	**0.89**	**0.83**	−0.06	0.16	0.00	**0.81**	0.13	**0.59**	**−0.61**	−0.20	1.00	
F$^-$	0.00	<u>0.25</u>	−0.11	−0.14	−0.21	**0.48**	0.20	−0.12	−0.02	<u>0.25</u>	0.16	**0.57**	−0.04	**−0.34**	1.00

Bold indicates correlation significance at the 0.01 level, and underlined means correlation significance at the 0.05 level
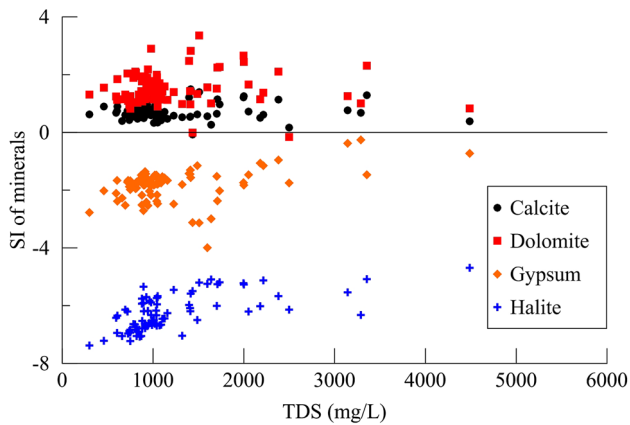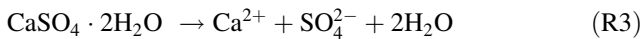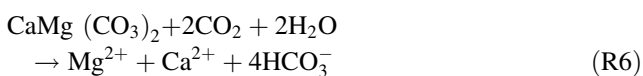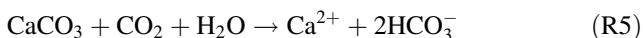
Fig. 6 Variation of saturation indices of selected minerals

from the dissolution of Glauber's salt ($NaSO_4 \cdot 10H_2O$), a common evaporite in the area. The dissolution of Glauber's salt also elevates the content of Na^+ in groundwater (R4).

$$CaSO_4 \cdot 2H_2O \rightarrow Ca^{2+} + SO_4^{2-} + 2H_2O \qquad (R3)$$

$$Na_2SO_4 \cdot 10H_2O \rightarrow 2Na^+ + SO_4^{2-} + 10H_2O \qquad (R4)$$
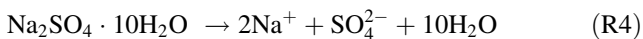
The relationship between $Ca^{2+} + Mg^{2+}$ and $SO_4^{2-} + HCO_3^-$ demonstrates the contribution of the dissolution of carbonates (such as calcite and dolomite) and sulfate minerals (such as gypsum) to groundwater chemistry. If the dissolution of carbonates and sulfate minerals is the sole source of these ions, plots should falls along the 1:1 line (Li 2014). As shown in Fig. 5c, most samples fall along the 1:1 line, signifying the contribution of the dissolution of carbonates and sulfate minerals to groundwater quality (R5 and R6). However, at the same time, majority of the samples fall above the 1:1 line in the $Ca^{2+} + Mg^{2+}$ versus HCO_3^- diagram (Fig. 5d), suggesting less contribution of Ca^{2+} by the dissolution of carbonates. The low correlations of HCO_3^- with Ca^{2+} and Mg^{2+} and high correlation between TH and SO_4^{2-} (Table 2) also support this statement. Furthermore, this is also evidenced by the saturation indices of calcite and dolomite which show that calcite and dolomite have already been oversaturated with respect to groundwater (Fig. 6), and no more these minerals can be dissolved in groundwater.

$$CaCO_3 + CO_2 + H_2O \rightarrow Ca^{2+} + 2HCO_3^- \qquad (R5)$$

$$CaMg(CO_3)_2 + 2CO_2 + 2H_2O \\ \rightarrow Mg^{2+} + Ca^{2+} + 4HCO_3^- \qquad (R6)$$
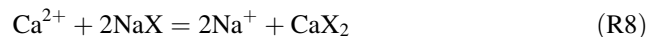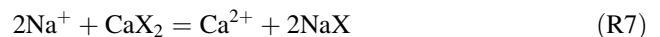
Cation Exchange

Cation exchange is another important natural process that can have significant impacts on the evolution of groundwater chemistry (Li et al. 2013a, b; Wu and Sun 2015). For studying the cation exchange occurring in groundwater system, two chloro-alkaline indices (CAI-1 and CAI-2) were proposed by Schoeller (Marghade et al. 2012; Schoeller 1965), which can be expressed as follows (Li et al. 2014d).

$$\text{CAI-1} = \frac{Cl^- - (Na^+ + K^+)}{Cl^-} \qquad (3)$$

$$\text{CAI-2} = \frac{Cl^- - (Na^+ + K^+)}{HCO_3^- + SO_4^{2-} + CO_3^{2-} + NO_3^-} \qquad (4)$$

where all ions are expressed in meq/L. If positive values for the two indices are obtained, cation exchange expressed as R7 occurs, and if negative values for them are achieved, reverse reaction takes place (R8). The calculation results of the two chloro-alkaline indices are plotted in Fig. 7a.

$$2Na^+ + CaX_2 = Ca^{2+} + 2NaX \qquad (R7)$$

$$Ca^{2+} + 2NaX = 2Na^+ + CaX_2 \qquad (R8)$$

The bivariate diagram between $(Na^+ + K^+ - Cl^-)$ and $[(Ca^{2+} + Mg^{2+}) - (HCO_3^- + SO_4^{2-})]$ (Fig. 7b) is also widely used for studying the possibility of cation exchange in groundwater (Ahmed et al. 2013; Li et al. 2016). $(Na^+ + K^+ - Cl^-)$ represents the increment of Na^+ induced by processes excluding halite dissolution, and $[(Ca^{2+} + Mg^{2+}) - (HCO_3^- + SO_4^{2-})]$ indicates the increment or decrement of Ca^{2+} and Mg^{2+} caused by processes excluding the dissolution/precipitation of gypsum, calcite, and dolomite (Farid et al. 2013; Li 2014). If cation exchange is a main process affecting groundwater salinity, the relationship between them should be linear and the slope close to -1 (Li 2014).

As shown in Fig. 7a, Most of the water samples in the study area fall in the lower left corner of Fig. 6a, indicating that most of the groundwater in the area has undergone reverse cation exchange expressed as R8. The cation exchange process increases the Na^+ content, while decreases the Ca^{2+} content in groundwater. However, Fig. 6a also shows that several water samples have undergone cation exchange expressed as R7, which is determined by specific hydrogeological and hydrogeochemcial environment. Figure 7b shows that the relationship of $(Na^+ + K^+ - Cl^-)$ and $[(Ca^{2+} + Mg^{2+}) - (HCO_3^- + SO_4^{2-})]$ for water samples conforms the following linear formula (5):

$$Y = -0.893X - 0.325 \; r = 0.742, \qquad (5)$$

where the fitted slope of the linear formula is -0.893, being very close to the theoretical value of -1, indicating that cation exchange between Na^+, Ca^{2+} and Mg^{2+} have occurred in groundwater. However, the difference between the fitted slope and theoretical value also indicates that cation exchange is not the only factor affecting the
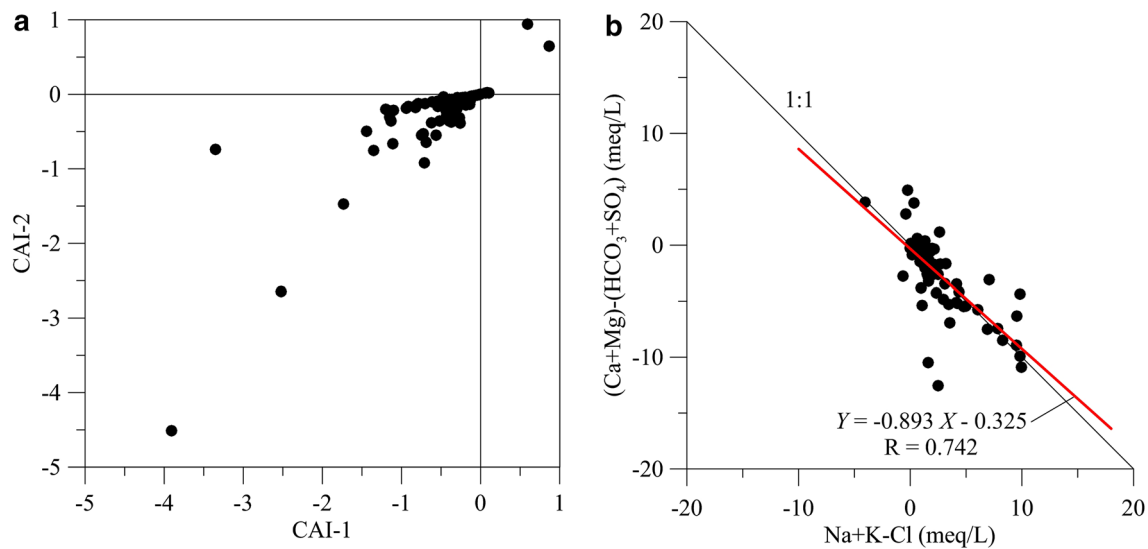
Fig. 7 Bivariate diagrams for studying cation exchange

concentrations of Na^+, Ca^{2+} and Mg^{2+} in groundwater, and their contents are also affected by other factors.

Evaporation

Evaporation is an important process influencing groundwater chemistry in the study area, especially in the alluvial plain. The isotopic relationship of δ^2H and $\delta^{18}O$ for shallow groundwater in the study area is shown in Fig. 8a. As shown in Fig. 8a, shallow groundwater in the study area falls below the local meteoric water line (LMWL) established by Qian et al. (2013), indicating strong evaporation of groundwater in the study area. Shallow groundwater samples conform to a groundwater evaporation line (GEL) expressed by Eq. (6).

$$\delta^2H = 3.89\delta^{18}O - 30.99 \qquad (6)$$

The GEL has a smaller slope than the LMWL, because evaporation tends to enrich heavy isotopes in waters (Qian et al. 2013). However, water–rock interactions have rare influences on their compositions below 60 °C if there is no evaporation, and isotopic compositions of groundwater can remain relatively stable (Qian et al. 2012b). This means that groundwater salinity due to evaporation can result in simultaneous increase in heavy isotopes. The GEL intersects LMWL at (-10.96, -73.62), and the values of -10.96 and -73.62 are estimated as baseline values for δ^2H and $\delta^{18}O$ in recharging rainfall, respectively (Fig. 8b, c). If samples are plotted above the lines, significant groundwater evaporation process can be confirmed. It is observed that all samples are plotted above the baselines (Fig. 8b, c) and this demonstrates that

evaporation has significant contribution to groundwater salinity.

Human Activities

Groundwater quality variation due to human activities is a complex process that is difficult to interpret, because it involves too many factors and uncertainties. As NO_3^- is widely recognized as a contaminant from human activities such as fertilizer application and domestic wastes, its relationships with physiochemical indices were used to interpret the impacts of human activities on groundwater quality in this study. As shown in Fig. 9a, the correlation between NO_3^- and Cl^- confirms the similar source of the two ions (Marghade et al. 2012; Li et al. 2016). Cl^- is significantly influenced by wastewater in addition to halite dissolution, it is, therefore, logical to state that NO_3^- is also influenced by wastewater. This is supported by the high concentration of NO_3^- in wastewater (Zheng et al. 2014). The positive correlation of TDS with (NO_3^- + Cl^-)/HCO_3^- (Fig. 9b) also supports the anthropogenic inputs to groundwater (Marghade et al. 2012). The study area has a long history of agriculture and fertilizer application is prevalent in this area to guarantee the crop productivity. Therefore, NO_3^- pollution is a common phenomenon here. Serious nitrite pollution and nitrate pollution have previously been reported in this area (Zhang et al. 2012).

The above discussions show that groundwater in the study area is influenced by both natural and anthropogenic factors. These factors are interrelated, making the chemical evolution of groundwater complex. It, therefore, calls for

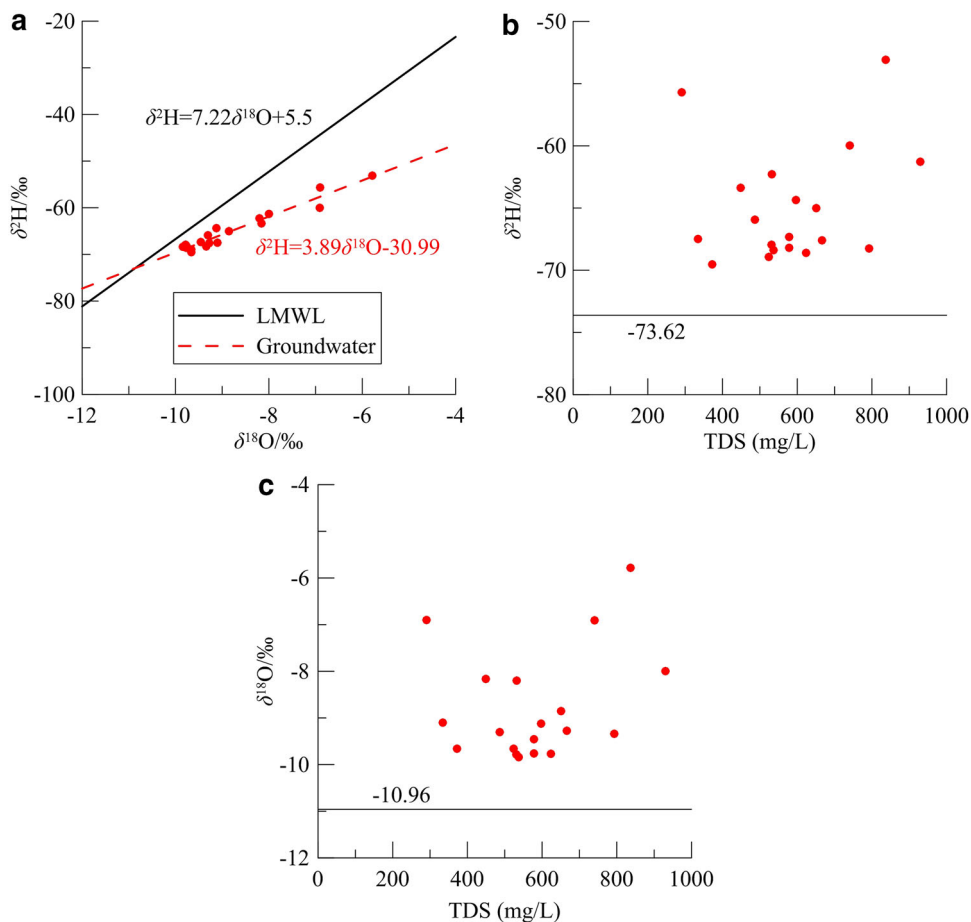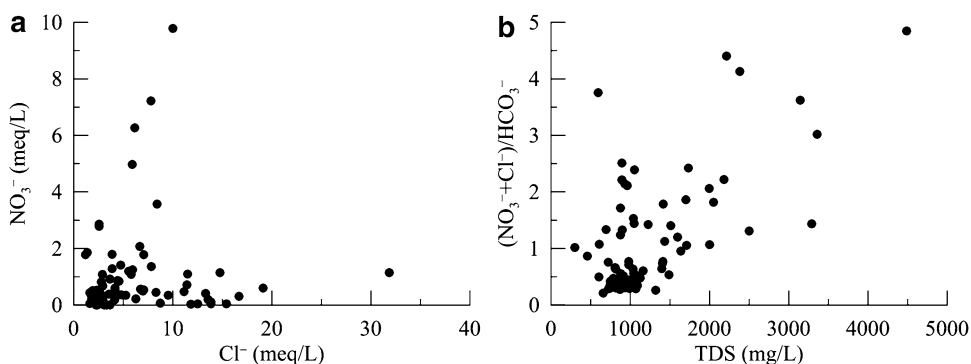**Fig. 8** Isotopic relationships of groundwater in the study area

Fig. 9 Relationships between NO_3^- and Cl^-/TDS

more comprehensive research in this field and more scholars to devote to it.

Hydrogeochemical Modeling

Although influenced by human activity, water–rock interaction is assumed to be the principal mechanism for the evolution of water chemistry. Hydrogeochemical modeling was performed with PHREEQC (Parkhurst and Appelo 1999). According to regional hydrogeology and

mineral content analyses, the following minerals are considered as the possible mineral phases for the geochemical modeling: calcite, albite, dolomite, gypsum, halite, quartz, fluorite, K-feldspar, kaolinite, anorthite, illite, chlorite, and kaolinite. As the phreatic groundwater system is an open system, CO_2 is considered for the simulation. Cation exchange between Na^+ and Ca^{2+} is also taken into account as it is an important process in the phreatic groundwater system (Li et al. 2014b). The same flow path as indicated in Fig. 1 was selected for the simulation.

Table 3 lists the mole transfers of phases calculated by PHREEQC.

For the upper section of the flow path (from N01 to N08), the dissolution of anorthite increases the concentration of Ca^{2+}, while the precipitation of calcite as well as cation exchange forces the decline of Ca^{2+} concentration along the path. The cation exchange increases Na^+ concentration, but the precipitation of albite lowers its concentration. As a consequence, the Na^+ concentration declines along the flow path from N01 to N08. Along the path from N01 to N08, K-feldspar dissolves, but the precipitation of illite balances the increase of K^+ in groundwater. Besides, the involvement of CO_2 enhances the dissolution of minerals. Overall, the precipitation of calcite, albite and illite, the dissolution of K-feldspar, anorthite, chlorite, and CO_2, as well as cation exchange between Na^+ adsorbed on the particle surface and Ca^{2+} in the solution, are the main water–rock interactions influencing groundwater chemistry in the desert region. Hydrochemical type transits from Cl–Ca to $HCO_3 \cdot SO_4$–Ca types.

Water–rock interactions for the lower section of the flow path (from N08 to S016) show some small differences from that of flow path from N01 to N08. Hydrochemical type changes from $HCO_3 \cdot SO_4$–Ca to $HCO_3 \cdot SO_4$–Ca·Mg types. The dissolution of halite is the main process explaining the increase of Na^+ and Cl^- in groundwater, while the dissolution of chlorite is the reason responsible for the increased Mg^{2+} concentration in groundwater. The dissolution of anorthite and gypsum is responsible for the elevation of

Ca^{2+} concentration, forcing the precipitation of dolomite. In addition, the dissolution of anorthite induces the precipitation of kaolinite (Qian et al. 2012b), which can be expressed by chemical equation (R9). The involvement of CO_2 can accelerate this process.

$$CaAl_2Si_2O_8 + 3H_2O + 2CO_2 \\ \rightarrow Al_2Si_2O_5(OH)_4 + Ca^{2+} + 2HCO_3^- \qquad (R9)$$
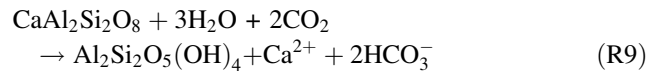
The differences between the water–rock interactions occurred in the two sections of the flow path should be attributed to different geologic and hydrogeologic conditions in these two sections. The hydrogeochemical modeling demonstrates that water–rock interactions are the dominant factors regulating groundwater chemistry in this area. The reaction rate and intensity, however, are influenced by climate and human activities.

Conclusions

Groundwater is an important source of water for various purposes in arid and semiarid regions. In the present study, Statistical analysis, graphical approaches, isotopic techniques, and hydrogeochemical modeling were applied to investigate the hydrochemical characteristics and the major factors influencing its evolution. The following conclusions can be reached.

- Statistical analysis demonstrates that the abundance of cations for groundwater in the study area follows the following order: $Na^+ > Ca^{2+} > Mg^{2+} > K^+$, while the abundance of anions for groundwater in the desert region is $HCO_3^- > Cl^- > SO_4^{2-}$, and that for groundwater in the alluvial plain is $HCO_3^- > SO_4^{2-} > Cl^-$. About half of the water samples are fresh water with TDS less than 1000 mg/L. HCO_3^- is the main anion for fresh water. Groundwater in the study area is mainly of HCO_3–Ca·Mg, SO_4–Na, $HCO_3 \cdot Cl$–Na·Ca, $HCO_3 \cdot SO_4 \cdot Cl$–Na·Mg types. The concentrations of physiochemical parameters in the desert region are usually higher than those in the alluvial plain partially because of the impacts of wastewater irrigation.
- Gibbs diagrams indicate that groundwater chemistry in the study area is mainly of rock dominance, with evaporation a significant influencing factor. Correlation analysis and graphic interpretation show that cation exchange and rock weathering such as dissolution of halite, albite, and carbonate minerals are important water–rock interactions governing the formation of groundwater chemistry. Stable isotopes suggest that shallow groundwater evaporation has occurred in the area and it is an important factor influencing groundwater quality. The occurrence of nitrate and its

Table 3 Mineral transfer amount calculated by PHREEQC (unit: mmol/L)

Phases	Chemical expression	Simulation path	
		N01-N08	N08-S016
Calcite	$CaCO_3$	−8.716	–
Albite	$NaAlSi_3O_8$	−0.274	−0.934
Dolomite	$CaMg(CO_3)_2$	–	−7.319
Gypsum	$CaSO_4{:}2H_2O$	−0.003	1.254
Halite	$NaCl$	–	1.496
Quartz	SiO_2	–	–
Fluorite	CaF_2	0.011	0.014
K-feldspar	$KAlSi_3O_8$	6.572	−0.019
Kaolinite	$Al_2Si_2O_5(OH)_4$	–	−9.781
Anorthite	$CaAl_2Si_2O_8$	8.900	8.351
Illite	$K_{0.6}Mg_{0.25}Al_{2.3}Si_{3.5}O_{10}(OH)_2$	−10.950	–
Chlorite	$Mg_5Al_2Si_3O_{10}(OH)_8$	0.548	1.906
CO_2 (g)	CO_2	8.763	20.950
NaX	NaX	0.273	–
CaX_2	CaX_2	−0.136	–

relationship with ions show that human activities have negative impacts on groundwater quality.

- Hydrochemical type, indicated by Piper and Stiff diagram, transits from Ca–Cl to $HCO_3 \cdot SO_4$–Ca and then to $HCO_3 \cdot SO_4$–Ca·Mg type along the flow path under the integrated impacts of natural factors and human activities. Although the groundwater chemistry is still of rock dominance, its natural property has already been gradually weakened and human interference begins to act as a significant role in influencing shallow groundwater quality.

- Hydrogeochemical modeling reveals that water–rock interactions for the upper and lower sections of the flow path show some small differences. For the upper section of the flow path, the precipitation of calcite, albite and illite, the dissolution of K-feldspar, anorthite, chlorite, and CO_2, as well as cation exchange between Na^+ adsorbed on the particle surface and Ca^{2+} in the solution, are the main water–rock interactions influencing groundwater chemistry. However, the dissolution of halite, chlorite, anorthite, and gypsum, and the precipitation of dolomite and kaolinite are the major water–rock interactions responsible for the variations of ions in shallow groundwater in the lower section of the flow path. The differences should be attributed to different geologic and hydrogeologic conditions in these two sections.

Compliance with Ethical Standards

Conflict of Interest The authors declare that they have no conflict of interest.

References

Ahmed MA, Abdel Samie SG, Badawy HA (2013) Factors controlling mechanisms of groundwater salinization and hydrogeochemical processes in the Quaternary aquifer of the Eastern Nile Delta, Egypt. Environ Earth Sci 68(2):369–394. doi:10.1007/s12665-012-1744-6

Ambast SK, Tyagi NK, Raul SK (2006) Management of declining groundwater in the Trans Indo-Gangetic Plain (India): some options. Agric Water Manag 82:279–296. doi:10.1016/j.agwat.2005.06.005

Ayotte JD, Belaval M, Olson SA, Burow KR, Flanagan SM, Hinkle SR, Lindsey BD (2015) Factors affecting temporal variability of arsenic in groundwater used for drinking water supply in the United States. Sci Total Environ 505:1370–1379. doi:10.1016/j.scitotenv.2014.02.057

Bouzourra H, Bouhlila R, Elango L, Slama F, Ouslati N (2015) Characterization of mechanisms and processes of groundwater salinization in irrigated coastal area using statistics, GIS, and hydrogeochemical investigations. Environ Sci Pollut Res 22:2643–2660. doi:10.1007/s11356-014-3428-0

Brindha K, Neena Vaman KV, Srinivasan K, Sathis Babu M, Elango L (2014) Identification of surface water–groundwater interaction by hydrogeochemical indicators and assessing its suitability for drinking and irrigational purposes in Chennai, Southern India. Appl Water Sci 4:159–174. doi:10.1007/s13201-013-0138-6

Candela L, Fabregat S, Josa A, Suriol J, Vigués N, Mas J (2007) Assessment of soil and groundwater impacts by treated urban wastewater reuse. A case study: application in a golf course (Girona, Spain). Sci Total Environ 374:26–35. doi:10.1016/j.scitotenv.2006.12.028

Chebotarev II (1955) Metamorphism of natural waters in the crust of weathering-1. Geochim Cosmochim Acta 8(1–2):22–48. doi:10.1016/0016-7037(55)90015-6

Chen J, Taniguchi M, Liu G, Miyaoka K, Onodera S, Tokunaga T, Fukushima Y (2007) Nitrate pollution of groundwater in the Yellow River delta, China. Hydrogeol J 15:1605–1614. doi:10.1007/s10040-007-0196-7

Christou A, Eliadou E, Michael C, Hapeshi E, Fatta-Kassinos D (2014) Assessment of long-term wastewater irrigation impacts on the soil geochemical properties and the bioaccumulation of heavy metals to the agricultural products. Environ Monit Assess 186:4857–4870. doi:10.1007/s10661-014-3743-4

Currell M, Cartwright I, Raveggi M, Han DM (2011) Controls on elevated fluoride and arsenic concentrations in groundwater from the Yuncheng Basin, China. Appl Geochem 26:540–552. doi:10.1016/j.apgeochem.2011.01.012

Durov SA (1948) Classification of natural waters and graphic presentation of their composition. Dokl Akad Nauk SSSR 59(1):87–90

El-Naqa A, Al-Shayeb A (2009) Groundwater protection and management strategy in Jordan. Water Resour Manage 23:2379–2394. doi:10.1007/s11269-008-9386-x

Esmaeili A, Moore F, Keshavarzi B (2014) Nitrate contamination in irrigation groundwater, Isfahan, Iran. Environ Earth Sci 72:2511–2522. doi:10.1007/s12665-014-3159-z

Fang J-J, Zhou A-G, Ma C-M, Liu C-F, Cai H-S, Gan Y-Q, Liu Y-D (2015) Evaluation of nitrate source in groundwater of southern part of North China Plain based on multi-isotope. J Cent South Univ 22:610–618. doi:10.1007/s11771-015-2562-2

Farid I, Trabelsi R, Zouari K, Abid K, Ayachi M (2013) Hydrogeochemical processes affecting groundwater in an irrigated land in Central Tunisia. Environ Earth Sci 68:1215–1231. doi:10.1007/s12665-012-1788-7

Gibbs RJ (1970) Mechanisms controlling world water chemistry. Science 17:1088–1090. doi:10.1126/science.170.3962.1088

Goyal MR, Tripathi VK (2016) Wastewater management for irrigation: principles and practices. Apple Academic Press, Canada

Han Z (1998) Groundwater for urban water supplies in northern China—an overview. Hydrogeol J 6(3):416–420. doi:10.1007/PL00010968

Jang T, Jung M, Lee E, Park S, Lee J, Jeong H (2013) Assessing environmental impacts of reclaimed wastewater irrigation in paddy fields using bioindicator. Irrig Sci 31:1225–1236. doi:10.1007/s00271-013-0401-5

Jin J (2013) Study on early warning of groundwater environment under papermaking wastewater irrigation condition. Master Thesis, Chang'an University, Xi'an (**in Chinese**)

Karagüzel R, Irlayici A (1998) Groundwater pollution in the Isparta Plain, Turkey. Environ Geol 34(4):303–308. doi:10.1007/s002540050282

Kassa A, Gavrieli I, Yechieli Y, Vengosh A, Starinsky A (2005) The impact of freshwater and wastewater irrigation on the chemistry of shallow groundwater: a case study from the Israeli Coastal Aquifer. J Hydrol 300:314–331. doi:10.1016/j.jhydrol.2004.06.013

Li P (2014) Research on groundwater environment under human interferences: a case study from Weining plain, Northwest China. PhD Thesis, Chang'an University, Xi'an (**in Chinese**)

Li H, Shao X, Huang X, Liao L (2007) Advance of research on harm of sewage irrigation in farmland and solving countermeasures. Water Saving Irrig 32(2):14–17 (**in Chinese**)

Li P-Y, Qian H, Wu J-H, Ding J (2010) Geochemical modeling of groundwater in southern plain area of Pengyang County, Ningxia, China. Water Sci Eng 3(3):282–291. doi:10.3882/j.issn.1674-2370.2010.03.004

Li P, Wu J, Qian H (2012) Groundwater quality assessment based on rough sets attribute reduction and TOPSIS method in a semi-arid area, China. Environ Monit Assess 184(8):4841–4854. doi:10.1007/s10661-011-2306-1

Li P, Qian H, Wu J, Zhang Y, Zhang H (2013a) Major ion chemistry of shallow groundwater in the Dongsheng Coalfield, Ordos Basin, China. Mine Water Environ 32(3):195–206. doi:10.1007/s10230-013-0234-8

Li P, Wu J, Qian H (2013b) Assessment of groundwater quality for irrigation purposes and identification of hydrogeochemical evolution mechanisms in Pengyang County, China. Environ Earth Sci 69(7):2211–2225. doi:10.1007/s12665-012-2049-5

Li P, Wu J, Qian H (2014a) Effects of irrigation with paper wastewater on soil fertility. In: Proceeding of the 2014 International Conference on GIS and Resource Management (ICGRM 2014). DEStech Publications, Inc., pp 322–328. doi:10.13140/2.1.4661.3124

Li P, Wu J, Qian H (2014b) Hydrogeochemistry and quality assessment of shallow groundwater in the southern part of the Yellow River Alluvial Plain (Zhongwei Section), China. Earth Sci Res J 18(1):27–38. doi:10.15446/esrj.v18n1.34048

Li P, Qian H, Wu J, Chen J, Zhang Y (2014c) Zhang H (2014c) Occurrence and hydrogeochemistry of fluoride in shallow alluvial aquifer of Weihe River, China. Environ Earth Sci 71(7):3133–3145. doi:10.1007/s12665-013-2691-6

Li P, Wu J, Qian H, Lyu X, Liu H (2014d) Origin and assessment of groundwater pollution and associated health risk: a case study in an industrial park, northwest China. Environ Geochem Health 36(4):693–712. doi:10.1007/s10653-013-9590-3

Li P, Qian H, Howard KWF, Wu J (2015) Building a new and sustainable ''Silk Road economic belt''. Environ Earth Sci 74:7267–7270. doi:10.1007/s12665-015-4739-2

Li P, Wu J, Qian H (2016) Hydrochemical appraisal of groundwater quality for drinking and irrigation purposes and the major influencing factors: a case study in and around Hua County, China. Arab J Geosci 9(1):15. doi:10.1007/s12517-015-2059-1

Marghade D, Malpe DB, Zade AB (2012) Major ion chemistry of shallow groundwater of a fast growing city of Central India. Environ Monit Assess 184:2405–2418. doi:10.1007/s10661-011-2126-3

Masto RE, Chhonkar PK, Singh D, Patra AK (2009) Changes in soil quality indicators under long-term sewage irrigation in a subtropical environment. Environ Geol 56:1237–1243. doi:10.1007/s00254-008-1223-2

McCallum JL, Crosbie RS, Walker GR, Dawes WR (2010) Impacts of climate change on groundwater in Australia: a sensitivity analysis of recharge. Hydrogeol J 18:1625–1638. doi:10.1007/s10040-010-0624-y

Naseem S, Rafique T, Bashir E, Bhanger MI, Laghari A, Usmani TH (2010) Lithological influences on occurrence of high-fluoride groundwater in Nagar Parkar area, Thar Desert, Pakistan. Chemosphere 78:1313–1321. doi:10.1016/j.chemosphere.2010.01.010

Nel J, Xu Y, Batelaan O, Brendonck L (2009) Benefit and implementation of groundwater protection zoning in South Africa. Water Resour Manage 23:2895–2911. doi:10.1007/s11269-009-9415-4

Parkhurst DL, Appelo CAJ (1999). User's Guide to PHREEQC (Version 2)-A Computer Program for Speciation, Batch-Reaction, One-Dimensional Transport, and Inverse Geochemical Calculations. United States Geological Survey. Water Resources Investigations Report 99-4259, Washington DC

Piper AM (1944) A graphic procedure in the geochemical interpretation of water-analyses. Trans Am Geophys Union 25(6):914–928. doi:10.1029/TR025i006p00914

Qian H, Li P (2011) Hydrochemical characteristics of groundwater in Yinchuan Plain and their control factors. Asian J Chem 23(7):2927–2938

Qian H, Li P, Howard KWF, Yang C, Zhang X (2012a) Assessment of groundwater vulnerability in the Yinchuan Plain, Northwest China using OREADIC. Environ Monit Assess 184(6):3613–3628. doi:10.1007/s10661-011-2211-7

Qian H, Ma Z, Li P (2012b) Hydrogeochemistry, 2nd edn. Geologic Publishing House, Beijing (**in Chinese**)

Qian H, Li P, Wu J, Zhou Y (2013) Isotopic characteristics of precipitation, surface and ground waters in the Yinchuan plain, Northwest China. Environ Earth Sci 70:57–70. doi:10.1007/s12665-012-2103-3

Qian J, Wang L, Liu Y, Wu B, Wang X (2015) Distribution of nitrate and its implication for the contaminant source in groundwater of Huaibei Plain, Anhui Province. Geosci J 19(3):537–545. doi:10.1007/s12303-014-0051-5

Rajesh R, Brindha K, Elango L (2015) Groundwater quality and its hydrochemical characteristics in a shallow weathered rock aquifer of southern India. Water Qual Expo Health 7:515–524. doi:10.1007/s12403-015-0166-6

Rattray G (2015) Geochemical evolution of groundwater in the Mud Lake area, Eastern Idaho, USA. Environ Earth Sci 73(12):8251–8269. doi:10.1007/s12665-014-3988-9

Rice EW, Baird RB, Eaton AD, Clesceri LS (2012) Standard methods for the examination of water and wastewater, 22nd edn. American Public Health Association, Washington DC

Sajil Kumar PJ, Elango L, James EJ (2014) Assessment of hydrochemistry and groundwater quality in the coastal area of South Chennai, India. Arab J Geosci 7:2641–2653. doi:10.1007/s12517-013-0940-3

Salem ZE, Atwia MG, El-Horiny MM (2015) Hydrogeochemical analysis and evaluation of groundwater in the reclaimed small basin of Abu Mina, Egypt. Hydrogeol J 23:1781–1797. doi:10.1007/s10040-015-1303-9

Sarikhani R, Dehnavi AG, Ahmadnejad Z, Kalantari N (2015) Hydrochemical characteristics and groundwater quality assessment in Bushehr Province, SW Iran. Environ Earth Sci 74:6265–6281. doi:10.1007/s12665-015-4651-9

Schacht K, Marschner B (2015) Treated wastewater irrigation effects on soil hydraulic conductivity and aggregate stability of loamy soils in Israel. J Hydrol Hydromech 63(1):47–54. doi:10.1515/johh-2015-0010

Schacht K, Chen Y, Tarchitzky J, Lichner L, Marschner B (2014) Impact of treated wastewater irrigation on water repellency of Mediterranean soils. Irrig Sci 32:369–378. doi:10.1007/s00271-014-0435-3

Schlager E (2006) Challenges of governing groundwater in U.S. western states. Hydrogeol J 14:350–360. doi:10.1007/s10040-005-0012-1

Schoeller H (1965) Qualitative evaluation of groundwater resources. In: Methods and techniques of groundwater investigation and development. Water Research Series-33. UNESCO, Delft, pp 54–83

Shurvilin AV, Chernukha NI, Saad GB (2010) Effect of long-term urban wastewater irrigation on heavy metal contamination of soils under conditions of Egypt. Russ Agric Sci 36(6):452–454. doi:10.3103/S1068367410060170

Stiff HA Jr (1951) The interpretation of chemical water analysis by means of patterns. J Petrol Technol 3(10):15–17. doi:10.2118/951376-G

Tarchouna LG, Merdy P, Raynaud M, Pfeifer H-R, Lucas Y (2010) Effects of long-term irrigation with treated wastewater. Part I: evolution of soil physico-chemical properties. Appl Geochem 25:1703–1710. doi:10.1016/j.apgeochem.2010.08.018

Vaux H (2011) Groundwater under stress: the importance of management. Environ Earth Sci 62:19–23. doi:10.1007/s12665-010-0490-x

Vetrimurugan E, Elango L (2015) Groundwater chemistry and quality in an intensively cultivated river delta. Water Qual Expo Health 7:125–141. doi:10.1007/s12403-014-0133-7

Wang Z, Yang G, Chen X, Fe Y, Zhang F, Chen J (2008) Groundwater contamination caused by wastewater irrigation and its controlling countermeasures. Hydrogeol Eng Geol 35(3):99–103 (in Chinese)

World Health Organization (WHO) (2011) Guidelines for drinking-water quality, fourth edition. http://apps.who.int/iris/bitstream/10665/44584/1/9789241548151_eng.pdf. Accessed 4 Dec 2015

Wu J, Sun Z (2015) Evaluation of shallow groundwater contamination and associated human health risk in an alluvial plain impacted by agricultural and industrial activities. Expo Health, Mid-west China. doi:10.1007/s12403-015-0170-x

Wu X, Qian H, Yu D, Zhang Q, Yan Z, Wang W, Ji Y, Liu H, Mao Z, Zhao Q (2008) Investigation and assessment of rational allocation of groundwater resources in the Yinchuan Plain. Geologic Publishing House, Beijing (in Chinese)

Wu J, Li P, Qian H, Chen J (2013) Groundwater pollution in and around a paper wastewater-irrigated area, Northwest China. In: Proceedings of the 4th International Conference on Digital Manufacturing and Automation (ICDMA 2013). IEEE, pp 649–652. doi:10.1109/ICDMA.2013.154

Wu J, Li P, Qian H (2014) Using correlation and multivariate statistical analysis to identify hydrogeochemical processes affecting the major ion chemistry of waters: a case study in Laoheba phosphorite mine in Sichuan, China. Arab J Geosci 7(10):3973–3982. doi:10.1007/s12517-013-1057-4

Wu J, Li P, Qian H (2015) Hydrochemical characterization of drinking groundwater with special reference to fluoride in an arid area of China and the control of aquifer leakage on its concentrations. Environ Earth Sci 73(12):8575–8588. doi:10.1007/s12665-015-4018-2

Yang H, Abbaspour KC (2007) Analysis of wastewater reuse potential in Beijing. Desalination 212:238–250. doi:10.1016/j.desal.2006.10.012

Zhang Y, Qian H, Li P, Jin H, Wu J, Jin J, Liu H, Liu H, Xie B, Xi W, Xu M, Wang S, Ding Y, Han Z (2012) Research Report on Regional Environmental Condition and Capacity in the Meili Paper Industrial Park. Ningxia Center of Environmental Monitoring, Yinchuan (in Chinese)

Zhang X, Xu Z, Sun X, Dong W, Ballantine D (2013) Nitrate in shallow groundwater in typical agricultural and forest ecosystems in China, 2004–2010. J Environ Sci 25(5):1007–1014. doi:10.1016/S1001-0742(12)60139-9

Zhang F, Jin Z, Yu J, Zhou Y, Zhou L (2015) Hydrogeochemical processes between surface and groundwaters on the northeastern Chinese Loess Plateau: implications for water chemistry and environmental evolutions in semi-arid regions. J Geochem Explor 156:101–113. doi:10.1016/j.gexplo.2015.08.010

Zhao Y (2010) Effects of wastewater irrigation on soil and groundwater environment. Shanxi Hydrotech 1:6–8 (in Chinese)

Zheng Z, Xie L, Qian H, Ding F (2014) Prediction and assessment of groundwater environment risks in the Weining Plain. Sunshine Press of the Yellow River Publishing Media, Yinchuan (in Chinese). Statistical analysis of groundwater samples